

# ON AUSTENITE CONDITIONING AND RECRYSTALLIZATION CONTROL OF HIGHER GRADE LINEPIPE STEELS (X100) WITH NIOBIUM AND MOLYBDENUM ADDITIONS

S.V. Subramanian<sup>1</sup> and Y. Yang<sup>1,2</sup>

<sup>1</sup>McMaster University Department of Materials Science and Engineering,  
Hamilton, Canada

<sup>2</sup>University of Science and Technology Beijing  
Beijing, China

Keywords: Linepipe, X100, X120, Microstructure, Precipitation, EBSD, High Angle Boundaries, TEM, Segregation, Charpy Toughness, Niobium, Molybdenum, Grain Refinement, Phase Transformation, Atom Probe, HAZ, Recrystallization

## Abstract

In higher strength linepipe steels (API Grade X100), research on structure-property correlation studies has underscored the importance of control of the density and dispersion of crystallographic high angle boundaries, which are effective as micro-crack arresters to suppress brittle fracture, in addition to morphological microstructure design to impart high strength and fracture toughness associated with resistance to ductile fracture. The control of density and dispersion of high angle boundaries, in turn, requires: (i) austenite grain refinement prior to pancaking, (ii) large strain accumulation by suppressing static recrystallization through strain-induced precipitation of NbC with adequate Zener drag force (NbC precipitate) and solute drag (Nb dissolved in matrix) in order to prevent boundary break away, and (iii) adequate hardenability to promote transformation at low temperature under accelerated cooling conditions to produce a lath structure with high angle boundaries by a displacive rather than a diffusive mechanism. The role of niobium microalloying on austenite conditioning and recrystallization control will be discussed in the light of quantitative modeling of strain induced precipitation of NbC and its interaction with recovery, and the effect of Zener and solute drag on boundary mobility and recrystallization. In order to promote transformation of pancaked austenite within a low temperature window, alloying with molybdenum is found to be effective, as molybdenum operates synergistically with solute niobium to promote transformation at a low temperature to give a fine lath structure having a high density of high angle boundaries. A combination of techniques involving EBSD, HRTEM and atom probe was used to characterize morphological structure, selection of crystallographic variants, nano-scale precipitates and solute dispersion in API Grade X100 containing niobium and molybdenum addition. The concept of hierarchical control on the evolution of microstructure with high density and dispersion of high angle boundaries will be discussed to achieve the target domain size in higher strength linepipe steels, with emphasis on Nb-Mo design in the base chemistry.

## Background

Control of density and dispersion of high angle boundaries, which are super-imposed on the microstructural morphology, is the quintessential requirement for improving the fracture behavior of higher grade linepipe steels. Since high angle boundaries act as barriers to microcrack propagation, it should be possible in principle to control brittle fracture initiation if microcracks could be arrested by high angle boundaries before they could grow to attain the critical Griffith crack length to spread across the grains, in accordance with the Cottrell-Petch model for brittle fracture [1]. If the occurrence of cleavage planes with low fracture stress is coincident with the fracture path, it is to be expected that brittle fracture will be aided by such incidence of crystallographic orientation. Thus, it is essential to understand texture evolution when processing linepipe steels and its consequence on brittle fracture behavior of linepipes.

In an early work on the ductile to brittle transition temperature in a bainitic steel with high yield strength (700 MPa), Gladman and Pickering [2] showed that the Ductile Brittle Transition Temperature (DBTT) is raised by a coarse austenite grain size, but the mechanism was not clarified, see Figure 1. John Knott [3] suggested that grain boundaries of coarse austenite grains are invariably associated with coarse carbide particles, which could crack to nucleate brittle fracture that could grow to the Griffith crack length to spread across the grains. However, in low interstitial high strength linepipe steels, such coarse carbides are seldom observed. On the other hand, brittle fracture is promoted by a low density of high angle boundaries occurring in coarse austenite grains in the heat affected zone when using high heat input welding. These large austenite grains are associated with a large interspacing of high angle boundaries, which are too large to arrest growth of micro-cracks from a dislocation pile-up which consequently reaches the critical Griffith crack length to trigger brittle fracture in accordance with the Cottrell-Petch model for brittle fracture. This hypothesis underscores the importance of control of density and dispersion of high angle boundaries to suppress brittle fracture in the design and development of higher grade linepipe steels. Linepipe produced from thermo-mechanically processed microalloyed steels is prone to exhibiting unpredictable failure, characterized by transition from ductile to brittle fracture behavior in full scale burst testing of pipes. This is attributed to a high intensity of  $\{100\} \langle 110 \rangle$  texture component according to a recent study on burst testing of linepipe [4]. The objective of the present work is to characterize the morphological and crystallographic features of higher grade linepipe steels in order to correlate morphological structure, crystallographic features (texture and boundary misorientations) with strength and fracture behavior of linepipe steel plate and the HAZ region. The control of density and dispersion of high angle boundaries in X100 based on high molybdenum-low niobium design will be examined in comparison with a recent cost-effective development of X100 based on low molybdenum-higher niobium multi-phase design.

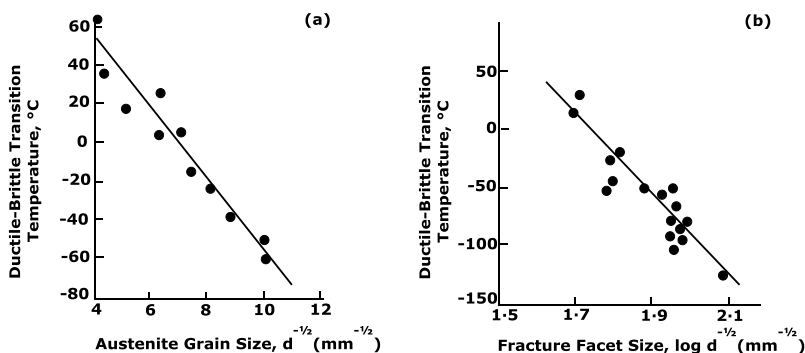


Figure 1. Effect of grain size on the ductile-brittle transition temperature in bainite-martensite structures; (a) effect of austenite grain size on a 700 MPa proof stress bainitic steel, (b) effect of fracture facet size in bainite-martensite structures, T. Gladman and F.B. Pickering [2].

## Experimental

The experimental work consisted of EBSD characterization of linepipe steels to generate a comprehensive data-base on the density and dispersion of high angle boundaries of steel samples thermo-mechanically processed under laboratory and industrial rolling conditions. The data-base comprises base chemistry, thermo-mechanical rolling parameters, pancaked austenite grain size as revealed by special metallographic etchants, EBSD characterization of density and dispersion of high angle boundaries in hot rolled plates and Gleeble samples subjected to thermal simulation of temperature cycles characteristic of HAZ region of welded plates, intensity of  $\{100\} \langle 110 \rangle$  texture from EBSD, and physical properties relating to strength and fracture behavior.

## Results

### EBSD Investigations on Bench-marked Higher Grade Linepipe Steels

Figure 2 shows a typical optical microstructure of pancaked austenite as revealed by metallographic etching of laboratory rolled and quenched HTP (High Temperature Processing) steel sample-B2. Figure 3 shows a band contrast map from EBSD of the corresponding region of the pancaked austenite grain. The variation in the density of high angle boundaries is mapped as a function of distance using line scans at any specific location in the pancaked austenite grain. The line scan closer to the pancaked austenite grain boundary is compared with two other locations in the interior of the austenite grain in Figure 3. It should be noted that only high angle boundaries above 35° are found to be effective in arresting cracks. The density (number count) of high angle boundaries with misorientations greater than 45° is high at the austenite grain boundary. The density of high angle boundaries decreases in the interior of the austenite grain. Thus in the middle of a large pancaked austenite grain, the interspacing of high angle boundaries is too large to arrest the growth of a micro-crack before it could reach the critical Griffith crack length for initiating brittle fracture. The crystallographic high angle boundaries associated with

microstructural constituents determine the domain size, which acts as the effective grain size of this complex optical microstructure in the Hall-Petch equation used to predict impact transition temperature. Table I summarizes sample identification, controlled rolling and accelerated cooling parameters, fracture behavior in DWTT (Drop-Weight Tear Test), impact toughness at  $-20\text{ }^{\circ}\text{C}$ , intensity of  $\{100\} \langle 110 \rangle$  texture component, and interspacing of high angle boundaries. Figure 4 is a plot of variation in the dispersion of average interspacing of high angle boundaries in the vicinity of austenite grain boundaries compared to the middle region of the austenite grain in different steel samples examined in this investigation.

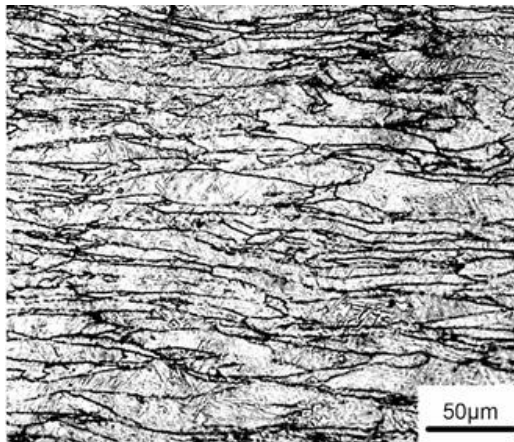


Figure 2. Optical microstructure of pancaked austenite grains in HTP steel sample-B2.

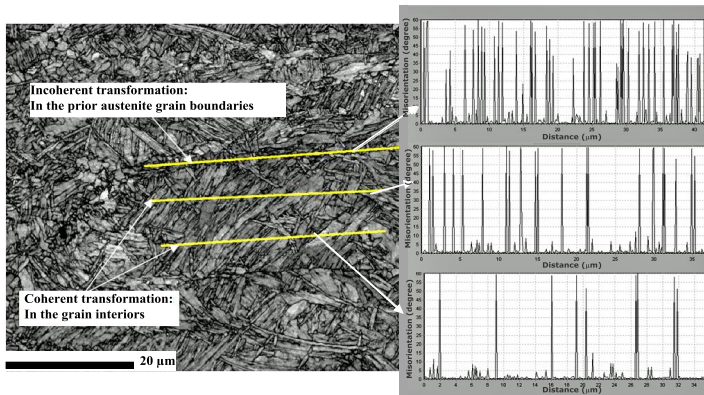


Figure 3. Band contrast map of sample-B2 plotting degree of misorientation along each line scan within a grain.

Table I. Compilation of Processing Parameters, Physical Properties, Texture, Prior Austenite Grain Size and Interspacing of High Angle Boundaries for Higher Niobium HTP (0.04%C, 0.095%Nb) Steels in Comparison with High Molybdenum-Nb-V Steels

Sample ID	Process			DWTT (SA%)	Average impact toughness at -20 °C (J)	{100}<011> Texture component (deviation = 20°)	Prior austenite grain size (microns)	Interspacing of high angle boundaries (>15 degree) (microns)	
	Deformation below T <sub>n</sub> r	Temp. of last pass (°C)	Cooling rate (°C/s)						
H T P	B1	61.7%	940	≥30	-	2.59%	<25	1.91	
	B2	61.7%	850	≥30	-	4.22%	<25	1.31	
	B3	61.7%	800	≥30	-	1.85%	<20	1.65	
	X90	62–67%	880–860	15–18	97% (-15 °C)	370	2.7%	<25	3
	W20	0		32		278	4.17%	<30	4.1
	W50	0		5.1		64	5.84%	>45	11.2
C (X100)	69%	790	35	95% (-15 °C)	174	2.44%	<25	2.10	
Large strain C1	80%	790	35		250	0.892%	<25	1.55	
B (X120) with boron	69%	790	34	100% (-15 °C)	178	0.205%	<25	1.30	

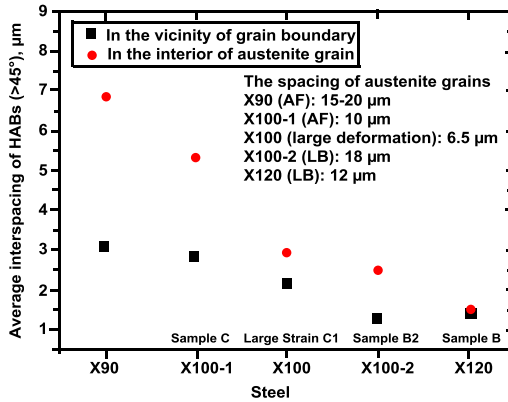


Figure 4. Average interspacing of high angle boundaries near the grain boundary and in the middle of pancaked austenite grains observed in different grades of linepipe steels.

Salient points from EBSD studies on base plates are summarized below:

- (i) The density and dispersion of high angle boundaries obtained in HTP sample B3, subjected to high cooling rate under laboratory conditions, are comparable to those obtained in high molybdenum, high vanadium low niobium sample C (X100). Recent industrial trials on HTP have confirmed the feasibility of producing X100 based on HTP chemistry by using large strain accumulation and a high cooling rate in excess of 25 °C/s.
- (ii) The effect of large strain accumulation combined with accelerated cooling is clearly to promote a high density of high angle boundaries as shown by mill rolled X90 based on HTP chemistry.
- (iii) The effect of increasing strain accumulation by increasing the total reduction below the no-recrystallization temperature,  $T_{nr}$ , from 69 to 80% in high Mo-Nb-V microalloyed steel of X100 grade is to increase the density of high angle boundaries and decrease the interspacing of high angle boundaries from 2.10 to 1.55 μm.
- (iv) The effect of boron addition to X100 is to promote X120 grade with a further increase in the density and uniformity of dispersion of higher angle boundaries. The structure exhibits a very low intensity of  $\{100\} \langle 110 \rangle$  texture and a domain size of less than 2 μm. More importantly, the structure exhibits a remarkable uniformity of dispersion of high angle boundaries and is associated with minimal variation in the interspacing of high angle boundaries from the grain boundary to the interior of austenite grain as shown in the plot in Figure 4.
- (v) In the absence of strain accumulation by prior deformation, the effect of a moderately low cooling rate (5 °C/s), characteristic of high heat input welding at 50 kJ/cm, “W-50”, is to promote a microstructure of granular bainite, which exhibits predominantly low angle misorientations ( $<10^\circ$ ). At a relatively high cooling rate (25 °C/s) corresponding to cooling schedules for low heat input welding of 20 kJ/cm, W-20, the microstructure is

lower bainite with a well delineated lath structure, which exhibits high angle misorientations ( $> 45^\circ$ ). The loss of toughness in higher heat input welding correlates with the loss of high angle boundaries in the HAZ region of HTP in W-50.

- (vi) A low intensity of (100)  $\langle 110 \rangle$  texture component is found to correlate well with a high density and uniform dispersion of high angle boundaries. The upstream refinement of austenite grains in X120 is remarkably good in producing pancaked austenite grains of less than  $10 \mu\text{m}$  thickness. High density and uniformity of dispersion of high angle boundaries causes the domain size to be less than  $2 \mu\text{m}$  in X120. The structure is coupled with low intensity {100}  $\langle 110 \rangle$  texture. Thus, the structure of X120 is identified as a target structure to aim for in order to control brittle fracture in higher grade linepipe steels.

### Control of Density and Dispersion of High Angle Boundaries

The functional role of niobium microalloying in API Grade X80 linepipe may be summarized as follows:

- (i) Strain induced precipitates of niobium carbo-nitride are used to pin austenite grain boundaries during thermo-mechanical rolling, which prevents recrystallization of austenite (by Zener drag).
- (ii) Niobium solute retards boundary mobility through solute drag and hence retards recrystallization. (Retardation of recrystallization of austenite by solute drag).
- (iii) Niobium retained in solid solution at the completion of finish rolling will aid in the formation of acicular ferrite upon accelerated cooling (Transformation hardening due to solute niobium in austenite).
- (iv) Upon transformation and holding at coiling temperature, the ferrite matrix is supersaturated with niobium and carbon that will result in fine precipitation of NbC in ferrite, which will contribute some additional strength by the precipitate hardening mechanism.

In higher grade linepipe steels such as X100 and X120, it has become essential to suppress competition from brittle fracture in niobium microalloyed steels. This warrants control of a high density and good dispersion of high angle boundaries, which, in turn, requires (i) austenite grain refinement prior to pancaking, (ii) large strain accumulation, by suppressing static recrystallization through strain-induced precipitation of NbC with adequate Zener drag force and solute drag due to niobium dissolved in the matrix in order to prevent boundary break away, and (iii) adequate hardenability, to promote transformation at low temperature under accelerated cooling conditions to produce lath structures with high angle boundaries by a displacive rather than a diffusion mechanism. These are examined in further detail below in three separate modules.

Module-1 Austenite Grain Refinement Prior to Pancaking. Grain refinement of austenite in upstream processing of HTP: Since a large interspacing of high angle boundaries associated with coarse austenite grains raises the DBTT, grain refinement of austenite before pancaking is an essential step to lower the DBTT well below the operating temperature of linepipes. Three potential strategies for grain refinement of austenite upstream are: (i) grain refinement by static or dynamic recrystallization, (ii) prevention of grain coarsening of austenite grains by upstream

precipitation of duplex precipitates of TiN and NbCN, and (iii) control of recrystallization nucleation kinetics by prior deformation.

Significant grain coarsening of austenite will occur in the high temperature window up-stream because of the thermodynamic driving force for reduction of surface energy by coarsening of austenite grains due to a capillarity effect, and high diffusion kinetics at elevated temperature. Grain coarsening of austenite can be counteracted by Zener pinning of boundaries by second phase particles. Recent work on X100 and X120 has confirmed that if a good dispersion of TiN particles is engineered in austenite, epitaxial growth of NbC will occur on pre-existing TiN particles, obviating the large undercooling associated with strain induced precipitation in upstream processing. These particles are found to be very effective in retarding the grain coarsening of austenite.

Analysis of an extensive data-base of DWTT results has underscored the importance of austenite grain refinement prior to pancaking. The laboratory research has led to the development of optimized high temperature processing (OHTP) of higher niobium steel for refining austenite grain size before pancaking. By imparting a deformation of 25% pass reduction at 1000 °C to a sample of HTP base chemistry with an initial average austenite grain size of 80 μm (from a prior deformation at 1070 °C), it is shown that recrystallized austenite grains are formed within seconds but these refined austenite grains do not coarsen significantly for up to 240 seconds of holding time [5]. It is further shown that niobium carbide precipitates are effective in stopping recrystallization fully for pancaking of austenite only below about 900 °C, and therefore there is significant potential for partial recrystallization in between these temperatures, particularly 960-920 °C. This can be safely avoided without grain coarsening of austenite by carrying out the last pass of roughing at 1000 °C and rapidly cooling within a short time to the start of finish rolling close to 900 °C. This is the metallurgical basis for austenite conditioning of higher niobium low molybdenum steel, particularly in modern mills with large capacity (10,000 tons) and the high productivity environment of thermo-mechanical rolling of heavy gauge (27 mm thick) and very wide (5000 mm) X80 plates using the higher niobium, low interstitial, HTP steel design.

#### Module-2 Strain Accumulation in Pancaked Austenite Grains During Controlled Rolling.

Physically based models are developed to analyze quantitatively time-evolution of strain induced precipitation of NbC during thermo-mechanical rolling for single pass deformation following the approach of Dutta and Sellars [6] and its interaction with recovery and recrystallization explicitly following the approach of Zurob et al. [7]. NbC precipitates nucleating on dislocations pin the dislocations impeding the recovery process. The effect of molybdenum is to delay the onset of strain induced precipitation, which allows recovery to precede strain induced precipitation, thereby lowering the driving force for recrystallization. Zurob's work has clarified that while strain induced precipitation occurs within a second or with a slight delay of 4-6 seconds with high Mn or Mo addition, the pinning of austenite boundaries takes a much longer time, involving tens of seconds for precipitates to grow adequately to exert the required Zener pinning force on boundaries to stop recrystallization. The model considers the time evolution of driving force for recrystallization, as influenced by Zener drag due to strain induced precipitates of NbC, and solute drag due to niobium dissolved in the matrix. The model for single pass deformation is the building block for multi-pass rolling. However, the phenomenology is rendered complex by

continuous fresh nucleation of precipitates on new dislocations during multi-pass rolling. More basic science work is in progress to capture recrystallization nucleation kinetics and growth in multi-pass rolling.

Stress relaxation has turned out to be a powerful technique for investigation of time evolution of strain induced precipitation and its interaction with recovery and recrystallization [8]. Previous work on stress relaxation studies in high niobium-high manganese steel by Banks et al. has shown that pinning of dislocations by nucleation of strain induced precipitates on dislocations impedes recovery at short times [9]. This has to be distinguished from Zener pinning of grain boundaries which occurs at much longer times, retarding recrystallization. Since the stored energy from dislocation density is the driving force for both recovery and recrystallization, physically based modeling is a valuable tool to interpret the results from coupling of recovery and recrystallization. The optimum design of base chemistry and rolling schedule is to control the strain induced precipitation kinetics to maximize the pinning force, while ensuring adequate solute niobium to prevent the boundary from breaking away from its solute atmosphere during finish rolling of niobium microalloyed steels [10].

Module-3 Transformation Control. Austenite with (i) large strain accumulation and (ii) adequate solute niobium, should be transformed under (iii) accelerated cooling conditions, to produce bainitic ferrite microstructures at low transformation temperatures in order to obtain a target domain size of about 2  $\mu\text{m}$  to meet X100 requirements. The scale of the bainitic microstructure decreases as the driving force for transformation and the strength of austenite are increased. One way of simultaneously increasing the driving force and the austenite strength is to reduce the transformation temperature as demonstrated by Bhadeshia and Singh [11]. In order to promote coherent transformation of pancaked austenite in a low temperature window, alloying with molybdenum and niobium is found to be effective. Molybdenum operates synergistically with solute niobium to promote transformation at low temperature to give a fine lath structure with a high density of high angle boundaries. The effect of molybdenum addition to niobium bearing higher strength linepipe grade steels on structure and properties is investigated by comparing high molybdenum-low niobium with higher niobium-low molybdenum alloy design.

#### Investigations of Structure and Properties of Nb-Mo Bearing Higher Grade Linepipe Steels

Table II shows the composition of high molybdenum, low niobium high V steel with and without boron addition. The base chemistry of the higher niobium low molybdenum multi-phase X100 steel is also included in Table II. The physical properties of the three steels are summarized in Table III.

Table II. Base Chemistry of Low Niobium (0.04%) - High Molybdenum (0.4%) Steels with and without Boron and Higher Niobium (0.08%) - Low Molybdenum (0.26%) Steel

Steel	C (wt%)	Mn (wt%)	B (ppm)	Nb (wt%)	V (wt%)	Mo (wt%)	N (ppm)	Remarks
Steel B Mo-Nb- V-B	0.041	1.6~1.7	8	0.038	0.069	0.4	47	X120
Steel C Mo-Nb- V	0.065	1.67	1	0.047	0.07	0.4	59	X100
Multi- phase 0.08 Nb- 0.25 Mo	0.07	1.75	-	0.081	-	0.26	≤ 40	X100 Multi-phase

Table III. Physical Properties of Low Niobium-High Molybdenum with and without Boron Compared to Higher Niobium-Low Molybdenum Multiphase Steel

Grade	R <sub>m</sub> (MPa)	R <sub>0.5</sub> (MPa)	Elongation A%	Avg. Charpy energy (J) at test temperature		Shear avg (%)
				-5 °C	241	
Steel B (X120) Mo-Nb-V-B [Nb 0.038, Mo 0.4, B 0.008]	907	810.6	16.75	-15 °C	178	100
				-5 °C	249	100
Steel C (X100) Mo-Nb-V [Nb 0.047, Mo 0.4]	792.9	690.6	19.5	-15 °C	174	95
				-5 °C	249	100
Multi phase (X100) Nb 0.081, Mo 0.26	909	708	(UEL 8) A-30	-20 °C	233	100

Previous work by Serin et al. [12] on nucleation kinetics of ferrite has shown that niobium is effective in inhibiting ferrite nucleation on austenite boundaries. The incubation time for ferrite nucleation is increased by a factor of 10 by niobium addition in C-Mn steel, which is comparable to that of boron. Niobium is also reported to decrease growth kinetics of ferrite by a factor of four compared to a reference C-Mn steel, which is attributed to interphase precipitation. Zhao et al. [13] have investigated the transformation characteristics of Mo-Nb-Cu-B low carbon steel under isothermal and continuous cooling conditions; molybdenum and niobium are shown to retard ferrite nucleation. The concept of hierarchical evolution of microstructure is used to promote multi-phase microstructures, comprising acicular ferrite at austenite grain boundaries by interrupted holding, and bainitic ferrite sheaves in the residual austenite matrix by quenching, in order to achieve adequate strength and toughness.

In the present investigation, in the absence of boron, a large reduction below  $T_{nr}$  (>70%) is required to ensure adequate strain accumulation to achieve X100 grade. Excellent strength with high density and dispersion of high angle boundaries are achieved with boron addition. The microstructure exhibits well pancaked austenite grains of uniform thickness of about 10  $\mu\text{m}$ . High angle boundaries occur between bainitic ferrite laths, which nucleate from austenite grain boundaries and extend to the middle of the austenite grains. Pole figure analysis has confirmed that high angle boundaries are formed between crystallographic units belonging to different Bain groups within each packet. The target structure for high toughness is characterized by well distributed packets within an austenite grain, and more importantly a large number of crystallographic units belonging to different Bain groups occurring within each packet, configured such that adjacent crystallographic units belong to different Bain groups. There is an optimum temperature window of transformation corresponding to an optimum cooling rate in which a large number of crystallographic units belonging to different Bain groups is obtained to give a high density of high angle boundaries. Hara et al. have shown the pronounced effect of niobium and molybdenum addition on lowering transformation temperature of low carbon bainitic steel containing boron [14]. At a cooling rate of 30  $^{\circ}\text{C}/\text{s}$ , the transformation temperature of boron containing steels is lowered by 50  $^{\circ}\text{C}$  with 0.04% niobium, and by 60  $^{\circ}\text{C}$  with 0.4% molybdenum addition respectively. Mohrbacher has provided a comprehensive review of the hardenability effect of molybdenum and niobium alloying in plate steels [15]. The refinement of austenite grain size prior to pancaking, a large reduction (>70%) below  $T_{nr}$  to promote a large Sv factor (grain boundary area per unit volume) in pancaked austenite with large strain accumulation and high cooling rates are demonstrated to be important processing parameters in low niobium-high molybdenum-high vanadium steels to achieve X100 properties.

#### High Resolution TEM Characterization of Micro-chemistry of Nano-scale Ti-Nb Precipitates in High Molybdenum – Low Niobium – High Vanadium Microalloyed X100 Steels

Ti-Nb microalloyed linepipe steels are designed for titanium rich nitride precipitation at elevated temperature. These precipitates are thermodynamically stable to pin austenite boundaries during high temperature excursions associated with high heat input welding in order to prevent austenite grain coarsening. Strain induced niobium rich carbide precipitates occur at relatively large undercooling (>100  $^{\circ}\text{C}$ ) during thermo-mechanical rolling, inhibiting recovery and recrystallization, thereby aiding strain accumulation [16]. If NbC grows epitaxially on pre-existing TiN particles, it will obviate the need for strain induced precipitation at large undercoolings. NbC will start growing at elevated temperature once the thermodynamic potential for precipitation occurs at the phase boundary. High resolution TEM has confirmed that in both X100 without boron addition and X120 with boron addition, a good dispersion of precipitates occurs. NbC grows on two opposite faces of cubic TiN precipitates exhibiting a dumb-bell appearance, as shown in Figure 5. The number density of the dumb-bell precipitates increases with boron addition. This finding is new and significant, as this can be used to advantage in austenite grain refinement prior to pancaking. These TiNb(CN) precipitates will retard the kinetics of grain coarsening of austenite in the HAZ region during high heat input welding.

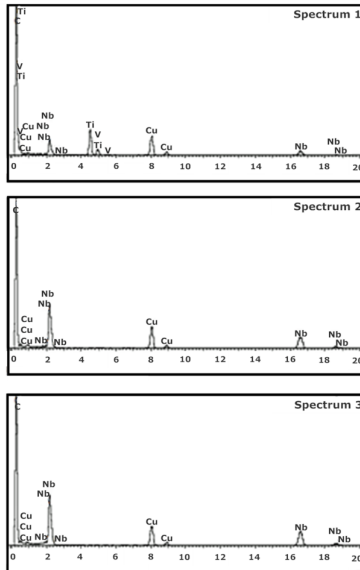
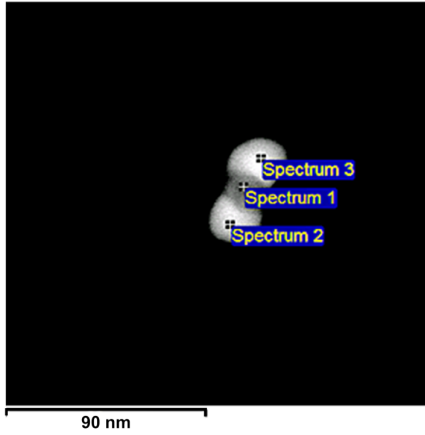


Figure 5. Ti-Nb nano-scale precipitate from X100 linepipe steel extracted by carbon replica. The middle spectrum shows a titanium rich phase. The top and bottom spectra show niobium rich phases attached to the two opposite faces of the cubic TiN.

## Atom Probe Results in High Molybdenum - Low Niobium - High Vanadium Microalloyed X100 Steel

In higher grade linepipe steel, strain accumulated pancaked austenite is rapidly cooled at 35 °C/s and the transformation occurs at a low temperature giving the lath structure. Under these conditions, it is believed that para-equilibrium holds with only carbon partitioning; by contrast, substitutional solutes like niobium do not partition as their diffusion coefficient is orders of magnitude lower than that of an interstitial solute like carbon. The residual austenite will be enriched in carbon, which could transform to hard and embrittling martensite, and the resulting hard MA product could initiate a microcrack. This phenomenon occurs in the heat affected zone, which promotes brittle fracture in the absence of crack arresters in the form of high angle boundaries. Atom probe examination has confirmed the occurrence of segregation of carbon at grain boundaries, but there is no segregation of substitutional solute, including niobium, at the grain boundaries. Atom probe analysis has also confirmed that niobium is evenly distributed in the matrix and there is no clustering of niobium. Figure 6 shows a map of carbon atoms as well as concentration profiles of solutes; both show significant segregation of carbon at the grain boundary. Figure 7 shows that the niobium distribution in the matrix is even. There is no evidence of niobium clusters in the matrix of the X100 linepipe that was examined [17].

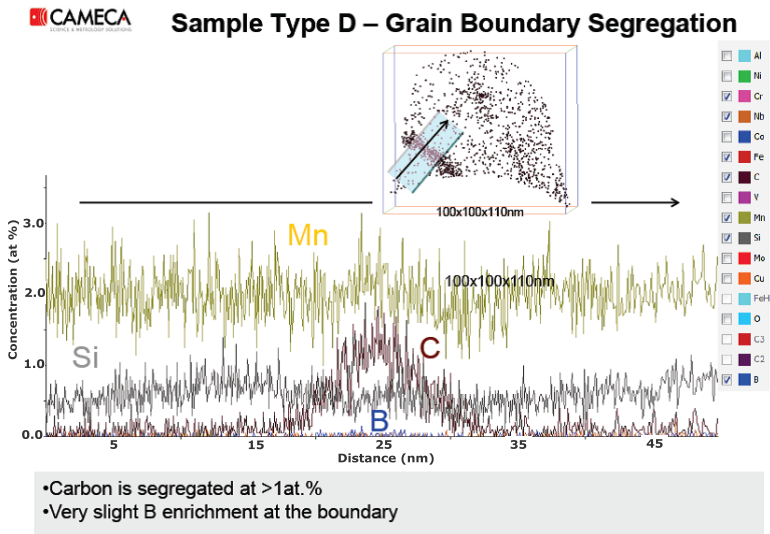
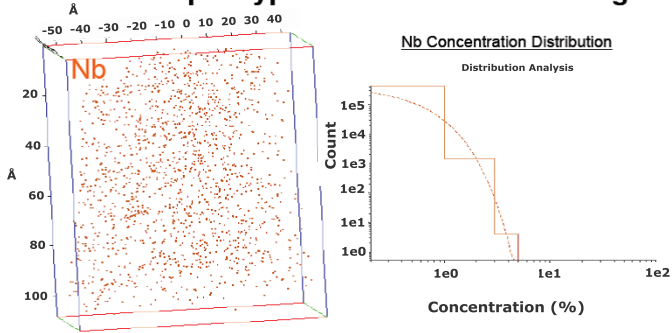


Figure 6. Atom map of carbon atoms (top) and concentration profiles of C, B, Si and Mn (bottom). Significant segregation of carbon was noted at the grain boundary.

## Sample Type D – Nb Clusters Testing



- In the dataset shown above, Nb is not clustered when compared with randomized data (dashed line)
- Small clusters observed visually in the data are not statistically different than expected random fluctuations

Figure 7. Niobium atom distribution with no clustering of niobium in the matrix.

### Development of X100 Based on Higher Niobium - Low Molybdenum Multi-phase Processing

The recent development of multi-phase X100 is a cost effective alloy design based on higher niobium - low molybdenum, which holds considerable promise. The approach is based on the concept of hierarchical evolution of microstructure by coherent transformation. The strategy is to adopt a two step processing: the first one is to interrupt and hold at the required temperature to promote an adequate amount of “ferrite” at austenite grain boundaries and the second process step is to quench and promote coherent transformation of austenite enriched in carbon to obtain bainitic ferrite. Figure 8 shows a typical microstructure of X100 from multi-phase processing of the higher niobium-low molybdenum chemistry.



Figure 8. Optical microstructure of multi-phase X100 based on low molybdenum (0.275%) higher niobium (0.08%).

#### Control of Density and Dispersion of High Angle Boundaries to Suppress Brittle Fracture in Single Pass HAZ of Multi-phase X100

The effect of heat input in single pass welding HAZ simulation on the toughness of the HAZ in higher niobium-low molybdenum multi-phase X100 was investigated. This provides a window of opportunity to study the hierarchical evolution of high angle boundaries as a function of cooling rate on a fixed, higher niobium-low molybdenum chemistry in coherent transformation of austenite without interference from dislocations due to deformation. Figure 9 shows Charpy impact toughness plotted as a function of heat input, SEM pictures of corresponding fracture surfaces, and a schematic diagram of different Bain groups from pole figure analysis, which are color coded. High angle boundaries occur between crystallographic units belonging to different Bain groups, which can be distinguished by interfaces of adjoining regions of two different colors. The one sample that exhibited ductile fracture showed a high density and dispersion of high angle boundaries, which occur within each packet, in addition to high angle boundaries occurring between the two adjoining packets within an austenite grain.

High angle boundaries within the packet are shown to occur between crystallographic units belonging to different Bain groups, whereas low angle boundaries occur between crystallographic units belonging to the same Bain group. Therefore, the target structure for a high density of high angle boundaries is identified as one where a high number density of crystallographic units belonging to different Bain groups occur within each packet and, more importantly, where the crystallographic units are arranged to maximize the interface between different Bain groups. Since bainitic ferrite laths belonging to different Bain groups nucleate on austenite grain boundaries, it is surmised that austenite grain size control is the key to promote a high density of high angle boundaries to suppress brittle fracture. This concept is also validated in X120 with a domain size of less than 2  $\mu\text{m}$ . In this case, the pancaked austenite size is of

5-10  $\mu\text{m}$  thickness, and high angle boundaries occur between bainitic ferrite nucleating from austenite grain boundaries and propagating to the middle of the pancaked austenite grains.

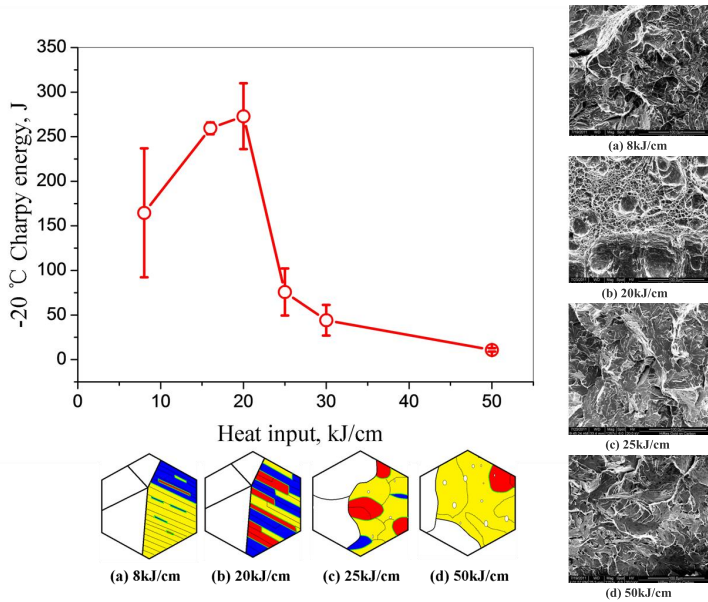


Figure 9. Charpy toughness at  $-20\text{ }^{\circ}\text{C}$  plotted against heat input; SEM fracture surface, and schematic of Bain groups occurring within a packet of austenite grain obtained for each of the four heat inputs examined. High angle boundaries occur between two distinctly different Bain groups as revealed by different color [18].

## Conclusions

1. High density and good dispersion of high angle boundaries are essential to suppress brittle fracture.
2. High angle boundaries are shown to form in the target structure between crystallographic units belonging to different Bain Groups occurring within each packet in an austenite grain, in addition to those formed between packets.
3. The control of density and dispersion of high angle boundaries in plate rolling requires: (i) austenite grain refinement prior to pancaking, (ii) large strain accumulation by large reduction below the temperature of no recrystallization  $T_{nr}$ , and (iii) adequate hardenability to promote transformation at low temperature under accelerated cooling conditions to produce a lath structure with high angle boundaries by the displacive rather than diffusive mechanism.
4. X100 based on high molybdenum-low niobium design: A high density of high angle boundaries can be obtained by increasing the hardenability of the base chemistry in X100. This can be achieved with a high molybdenum addition (0.4 wt%) to traditionally alloyed medium niobium (0.045 wt%) and 0.08%V steel. The steel is designed for thermo-mechanical rolling and accelerated cooling in a conventional mill.
5. However, newer X100 alloy and processing designs have emerged based on a higher niobium-low molybdenum multi-phase concept: X100 with a minimum of 6% uniform elongation to meet strain-based design is based on higher niobium (0.08%) and low molybdenum contents. Two step processing is used involving interrupted holding to promote ferrite at prior austenite grain boundaries and quenching the residual austenite to produce bainitic ferrite so as to produce a dual phase structure. This steel composition is the lowest cost design which exploits the advanced processing capabilities of a modern mill.

## Acknowledgements

The authors wish to thank Dr. Gianluigi Botton, Dr. Glynis de Silveira and Dr. Carmen Andrei for help with high resolution TEM, and Mr. Chris Butcher, BIMR for help with EBSD. The funding support by CBMM, Brazil is gratefully acknowledged.

The authors wish to thank (i) Chinese Government for the award of scholarships to You Yang to do research at McMaster University, (ii) Dr. Laurie Collins of Evraz Inc NA, Regina, Canada for research support, (iii) Sha Steel for supply of steels and technical support and (iv) Dr. Chengjia Shang, USTB, China for collaborative research.

## References

1. Alan Cottrell, "Brittle Fracture From Pile-ups in Polycrystalline Iron," *Yield, Flow and Fracture of Polycrystals*, ed. T.N. Baker (Applied Science Publishers, 1983), 123-129.
2. T. Gladman and F.B. Pickering, "Effect of Grain Size on the Mechanical Properties of Ferrous Materials," *Yield, Flow and Fracture of Polycrystals*, ed. T.N. Baker, (Applied Science Publishers, 1983), 141-198.
3. J.F. Knott, "Cleavage Fracture and the Toughness of Structural Steels," *Yield, Flow and Fracture of Polycrystals*, ed. T.N. Baker, (Applied Science Publishers), 81-99.
4. I. Psyhmintsey et al., "Effect of Microstructure and Texture on Shear Fracture in X80 Line Pipe Designed for 11.8 MPa Gas Pressure" (Paper presented at the Ostend Conference, November, 2009).
5. C.L. Miao et al., "Recrystallization and Strain Accumulation Behavior of High Niobium-bearing Linepipe Steel in Plate and Strip Rolling," *Materials Science and Engineering A*, 527 (2010), 4985-4992.
6. B. Dutta, E.J. Palmiere, and C.M. Sellars, "Modelling the Kinetics of Strain Induced Precipitation in Nb Microalloyed Steels," *Acta Materialia*, 49 (2001), 785.
7. H.S. Zurob et al., "Modeling Recrystallization of Microalloyed Austenite: Effect of Coupling Recovery, Precipitation and Recrystallization," *Acta Materialia*, 50 (2002), 3075.
8. C.L. Miao et al., "Refinement of Prior Austenite Grain in Advanced Pipeline Steel," *Frontiers Materials Science China*, 4 (2010), 197-201.
9. K.M. Banks et al., "High Temperature Processing and Accelerated Cooling of X65 Line Pipe Steel on a 4000T Plate Mill" (Paper presented in the Proceedings of the International Conference on Microalloying, Pittsburgh, June 2007).
10. H. Zurob et al., "Analysis of the Effect of Mn on the Recrystallization Kinetics of High Nb Steel: An Example of Physically Based Model," *The Iron and Steel Institute of Japan International*, 45 (5) (2005), 713-722.
11. S.B. Singh and H.K.D.H. Bhadeshia, "Estimation of Bainite Plate-thickness in Low-alloy Steels," *Materials Science and Engineering A*, 245 (1) (1998), 72-79.
12. B. Sarin et al., *Memoires Scientifiques de la Revue de Metallurgie*, June, 5, (1978), 355-369.
13. Y.T. Zhao et al., "The Metastable Austenite Transformation in Mo-Nb-Cu-B Low Carbon Steel," *Materials Science and Engineering A*, 433 (2006), 169-174.

14. T. Hara et al., "Role of Combined Addition of Niobium and Boron and of Molybdenum and Boron on Hardenability in Low Carbon Steels," *Iron and Steel Institute of Japan International*, 44 (8) (2004), 1431-1440.
15. H. Mohrbacher, "Mo and Nb Alloying in Plate Steels for High Performance Applications" (Paper presented at the Proceedings of the International Symposium on the Recent Developments in Plate Mill, AIST, Winter Park, Colorado 19-22 June 2011).
16. E.J. Palmiere, C.M. Sellars, and S.V. Subramanian, "Modeling of Thermomechanical Rolling" (Paper presented at the International Symposium Niobium 2001, AIME-TMS, Orlando, U.S.A, December 2001), 501- 526.
17. S.V. Subramanian et al., "Characterization of Nano-scale Precipitates in Microalloyed Steel" (Paper presented at the Proceedings of the International Conference: Advances on Analytical Techniques and Characterization of Materials (ATCOM), Ranchi, India, 5-7 July, 2011).
18. S.V. Subramanian et al., "EBSD Characterization of HAZ from Single and Multi-pass Welding of Niobium Microalloyed Line Pipe Steels" (Paper presented at the Proceedings of the TMS-CBMM Seminar on Welding of Pipeline Steels, Araxa, 28-29 November, 2011).